AUTOPHAGY
2020, VOL. 16, NO. 8, 1453–1467
https://doi.org/10.1080/15548627.2019.1687214

Taylor & Francis
Taylor & Francis Group

RESEARCH PAPER

Check for updates

BAG2 ameliorates endoplasmic reticulum stress-induced cell apoptosis in *Mycobacterium tuberculosis*-infected macrophages through selective autophagy

Shuxin Liang[a,b*], Fengyu Wang[a,b*], Changlei Bao[a,b], Jing Han[a,b], Ying Guo[a,b], Fayang Liu[a,b], and Yong Zhang[a,b]

[a]College of Veterinary Medicine, Northwest A&F University, Yangling, Shaanxi, China; [b]Key Laboratory of Animal Biotechnology, Ministry of Agriculture, Northwest A&F University, Yangling, Shaanxi, China

ABSTRACT

BAG2 (BCL2 associated athanogene 2) is associated with cell fate determination in response to various pathological conditions. However, the effects of BAG2 on *M. tuberculosis*-induced endoplasmic reticulum (ER) stress remain elusive. Herein, we report that *M. tuberculosis* infection of macrophages triggered ER stress and downregulated BAG2 expression. Overexpression of BAG2 enhanced autophagic flux and activated macroautophagy/autophagy targeted to the ER (reticulophagy). In addition, through increasingly localizing SQSTM1 to the ER in BAG2-overexpressing macrophages, we found that the autophagy receptor protein SQSTM1/p62 (sequestosome 1) is associated with the BAG2-induced reticulophagy. Our data also confirmed that BAG2 could render cells resistant to *M. tuberculosis*-induced cellular damage, and the anti-apoptotic effects of BAG2 in *M. tuberculosis*-treated macrophages were partially abolished by the autophagic flux inhibitor bafilomycin A_1. Furthermore, the dissociation of BECN1 and BCL2 mediated by activation of mitogen-activated protein kinase (MAPK)/extracellular signal-regulated kinase (ERK) was responsible for BAG2-activated autophagy. In addition, XBP1 downstream of the ERN1/IRE1 signaling pathway was bound to the *Bag2* promoter region and transcriptionally inhibited BAG2 expression. Collectively, these results indicated that BAG2 has anti-apoptotic effects on *M. tuberculosis*-induced ER stress, which is dependent on the promotion of autophagic flux and the induction of selective autophagy. We revealed a potential host defense mechanism that links BAG2 to ER stress and autophagy during *M. tuberculosis* infection.

Abbreviations: ATF6: activating transcription factor 6; BECN1: beclin 1; Baf A1: bafilomycin A_1; CASP3: caspase 3; DDIT3/CHOP/GADD153: DNA damage inducible transcript 3; DAPI: 4′,6-diamidino-2-phenylindole; EIF2AK3/PERK: eukaryotic translation initiation factor 2 alpha kinase 3; ER: endoplasmic reticulum; ERN1/IRE1: endoplasmic reticulum to nucleus signaling 1; HSPA5/GRP78/BiP: heat shock protein 5; MAP1LC3B/LC3B: microtubule associated protein 1 light chain 3 beta; MAPK/ERK: mitogen-activated protein kinase; SQSTM1/p62: sequestosome 1; UPR: unfolded protein response; XBP1: x-box binding protein 1

ARTICLE HISTORY
Received 5 March 2019
Revised 9 October 2019
Accepted 28 October 2019

KEYWORDS
Apoptosis; autophagy; BCL2 associated athanogene 2; endoplasmic reticulum stress; *M. tuberculosis*; reticulophagy

Introduction

BAG2 (BCL2 associated athanogene 2) is a member of the BAG family. As a group of multifunctional proteins, BAG proteins interact with numerous proteins and take part in diverse cellular processes, including cell division, cell death and differentiation [1]. Our previous study confirmed that BAG2 expression is modulated in *M. tuberculosis*-infected RAW264.7 cells [2] and interacts with SP110 (intracellular pathogen resistance 1 gene) [3], conferring resistance against *M. tuberculosis* [4]. We demonstrated that BAG2 also interacts with unphosphorylated STAT1, which represses apoptosis in macrophages during *M. tuberculosis* infection [5]. Recent studies showed that BAG2 inhibits apoptosis by decreasing the intracellular mature form of CTSB [6] and promotes tumorigenesis via increased mutant TRP53 accumulation [7]. These studies demonstrated that BAG2 expression correlates with cell survival. However, the effects of BAG2 on *M. tuberculosis*-mediated cell fate have not been established.

Endoplasmic reticulum (ER) stress is caused by accumulation of unfolded or misfolded proteins, hypoxia, oxidative stress, and bacterial infections. For instance, methicillin-resistant *Staphylococcus aureus* infection activates an ER stress sensor, ERN1/IRE1 (ER to nucleus signaling 1)-mediated ROS generation, to kill bacterial pathogens [8]. Similarly, mycobacterial infection also induces ER stress to regulate cellular and mycobacterial fates [9,10].

Autophagy, facilitating the degradation of damaged organelles and misfolded proteins [11,12], is recognized to play a key role in antimicrobial defense mechanisms [13]. Importantly, autophagy can both regulate host resistance against mycobacterial infections [14] and control cellular survival [15]. Recently, the BAG family has been shown to induce autophagy [16,17]. However, it remains to be resolved

CONTACT Yong Zhang zhangyong1956@nwafu.edu.cn College of Veterinary Medicine, Northwest A&F University, Yangling, Shaanxi 712100, China
*These authors contributed equally to this work.
Supplemental data for this article can be accessed here.
© 2019 Informa UK Limited, trading as Taylor & Francis Group

whether BAG2 can modulate autophagy in macrophages in order to regulate mycobacterial fates.

In this study, we demonstrated that BAG2 protects cells from ER stress-induced apoptosis and induces autophagy. This autophagy resolves ER stress by removing stressed ER membranes, a process termed reticulophagy [18], thereby protecting macrophages from infection-induced apoptosis. BAG2 activates autophagy by MAPK/ERK-mediated phosphorylation of BCL2 during *M. tuberculosis* infection. Additionally, XBP1 (X-box binding protein 1), which is downstream of the ERN1 pathway, suppresses transcriptional expression of *Bag2* in infected macrophages. These results implied that BAG2 plays a key and connective role between ER stress and autophagy in mediating antibacterial defenses.

Results

BAG2 expression is reduced under M. tuberculosis*-induced ER stress and BAG2 protects macrophages from apoptosis*

To examine if ER stress is induced during *M. tuberculosis* infection, we infected murine BMDMs and RAW264.7 cells with *M. tuberculosis* for the indicated times. As shown in Figure 1A and B, ER stress marker DDIT3 and HSPA5 increased during infection. Considering that the BAG family participates in ER stress [19,20], we investigated whether BAG2 expression is associated with *M. tuberculosis*-induced ER stress. We treated murine BMDMs and RAW264.7 cells with *M. tuberculosis* and pharmacological ER stress inducer (tunicamycin or thapsigargin) and found that BAG2 expression was downregulated in a time dependent manner upon activation of unfolded protein response (UPR) in both BMDMs and RAW264.7 cells (Figure 1A–D and Figure S1). Together, ER stress decreased BAG2 levels during *M. tuberculosis* infection.

Recent studies have suggested that *M. tuberculosis* can induce ER stress-mediated apoptosis [21,22]. We examined the effects of BAG2 on ER stress-triggered apoptosis after *M. tuberculosis* infection by knocking down *Bag2* via RNA interference. *Bag2* knockdown reduced viability of BMDMs and RAW264.7 cells upon infection (Figure 1E). Consistently, BAG2 overexpression enhanced survival of RAW264.7 and J744A.1 cells during infection (Figure 1F).

A previous report suggested that ER stress-mediated apoptosis influences the survival of mycobacteria within macrophages [23]. Thus, we examined whether BAG2 is related to intracellular survival of *M. tuberculosis*. To address this issue, we targeted *Bag2* by siRNA in BMDMs and RAW264.7 cells and assayed *M. tuberculosis* H37Ra survival by plating. Knockdown of *Bag2* increased mycobacteria elimination in infected cells (Figure 1G). Moreover, controls for possible detachment of macrophages showed that only 5%–7% of total input cells were detached, irrespective of treatment (Figure 1H).

BAG2 promotes autophagy and enhances autophagic flux in macrophages during M. tuberculosis *infection*

Autophagy promotes cell survival in response to ER stress [24–26]. Thus, we determined if BAG2-mediated protection of macrophages upon infection is related to activation of autophagy. First, we infected BMDMs and RAW264.7 cells with *M. tuberculosis* H37Ra and examined the kinetics of autophagosome formation by western blotting for LC3. As shown in Figure 2A–D and Figure S2, *M. tuberculosis* H37Ra induced autophagy in BMDMs and RAW264.7 cells before 24 h. To assess the role of BAG2 in *M. tuberculosis* H37Ra-induced autophagy, we first evaluated autophagic flux in BMDMs and RAW264.7 cells with interfering *Bag2* expression. Knockdown of *Bag2* diminished LC3-II expression in BMDMs and RAW264.7 cells (Figure 2B) and endogenous LC3 puncta formation in RAW264.7 cells (Figure 2E) after treatment with *M. tuberculosis* H37Ra. In contrast, BAG2 overexpression enhanced activation of autophagy (Figure 2D and E). We also examined whether BAG2 induced autophagosome-lysosome fusion by staining colocalization between LC3 and lysosomes. Confocal images showed that macrophages treated with *Bag2* siRNA decreased accumulation of the LC3 and lysosomes (stained with LysoTracker) (Figure 2F and G). These findings indicated that BAG2-induced autophagosomes are targeted and fuse with lysosomes. Addition of the vacuolar H+-ATPase inhibitor bafilomycin A_1 (Baf A1) lead to accumulation of the autophagic vesicle marker LC3-II, and *Bag2* siRNA decreased this accumulation (Figure 2H). Thus, BAG2 activates both autophagy and autophagosome-lysosome fusion during *M. tuberculosis* H37Ra infection. In addition, inhibition of autophagy did not influence downregulation of BAG2 in H37Ra-infected macrophages (Figure 2I).

BAG2 induces reticulophagy in macrophages during M. tuberculosis *infection*

Autophagy can relieve ER stress and attenuate ER stress-induced apoptosis, and parts of the ER can be degraded by autophagy, a process referred to as reticulophagy [27]. To determine whether BAG2 could activate autophagy targeted in the ER, double-labeled immunofluorescence staining was performed. The results showed that BAG2 enhances the colocalization of LC3 puncta and ER after infection, compared to control group (Figure 3A). Furthermore, we observed autophagosomes, autolysosomes and ER by transmission electron microscopy (TEM) after Baf A1 was used to treat BAG2-overexpressed RAW264.7 cells during infection. Compared to control group, BAG2 overexpression showed more autophagosomes and autolysosomes formation (Figure 3B). Meanwhile, zoom up views revealed that macrophages stimulated with H37Ra exhibited dilated ER, a morphology consistent with ER stress, and the autophagosomes contained parts of ER whorls in cells transfected with BAG2 plus Baf A1 (Figure 3B).

The interaction between BAG2 and SQSTM1 was required for reticulophagy during M. tuberculosis *infection*

Since SQSTM1 could act as an autophagy receptor for the autophagic removal of excess ER [28], we investigated the relationship of BAG2 and SQSTM1. The co-localization and co-IP assays of BAG2 with SQSTM1 showed that BAG2 binds to SQSTM1 in RAW264.7 cells (Figure 4A and C), suggesting

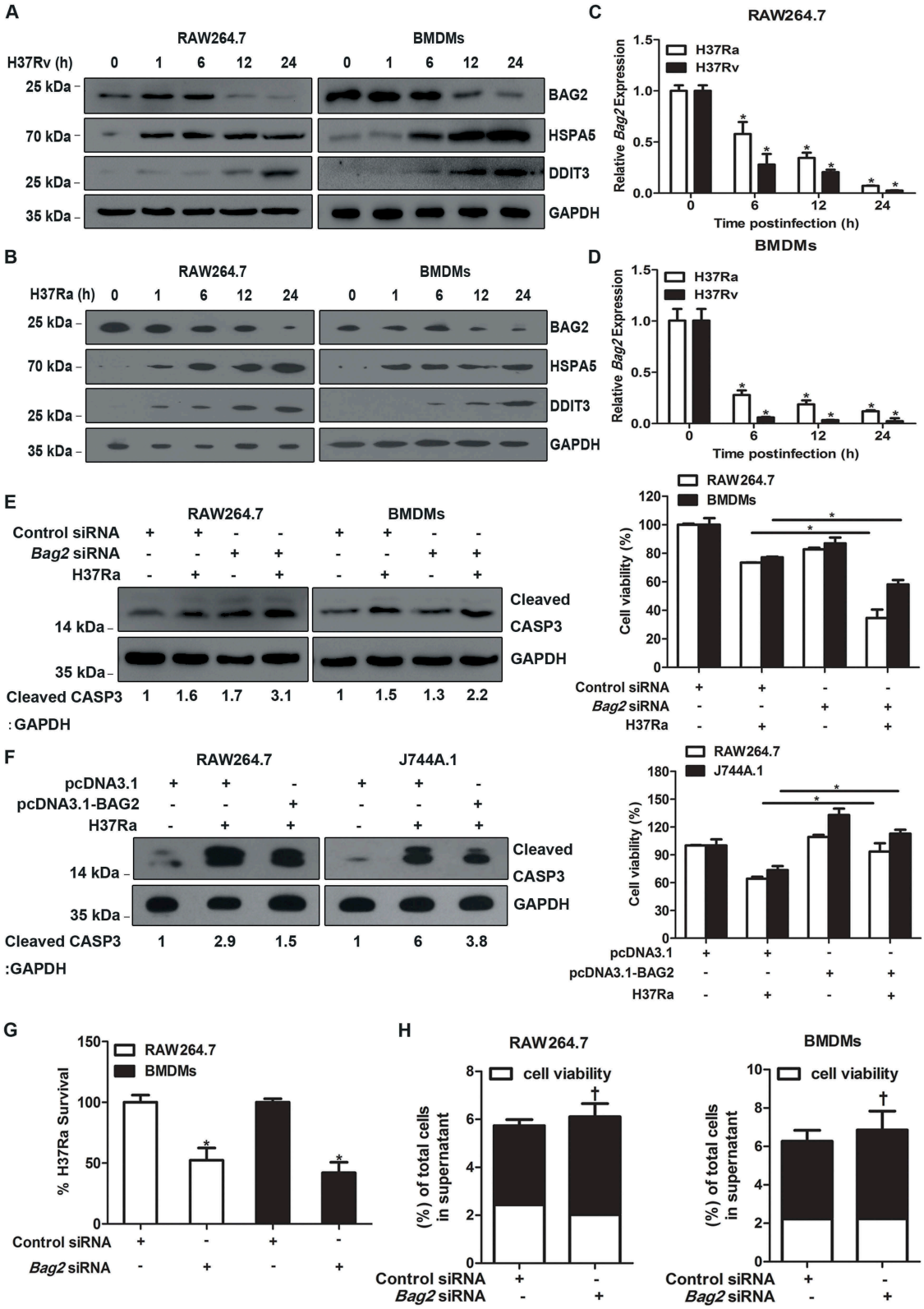

Figure 1. BAG2 is downregulated under *M. tuberculosis*-induced ER stress and decreases ER stress-induced apoptosis in murine macrophage cells. (A and B) RAW264.7 cells and BMDMs were infected with *M. tuberculosis* H37Rv (A) and H37Ra (B) for the indicated times. Expression levels of BAG2, HSPA5, DDIT3 and GAPDH were determined by western blot. (C and D) RAW264.7 cells (C) and BMDMs (D) were infected with *M. tuberculosis* H37Rv and H37Ra for the indicated times. Expression levels of *Bag2* were tested by qPCR. (E and F) RAW264.7 cells, J744A.1 cells and BMDMs were transfected with control siRNA or *Bag2* siRNA (E); control vectors or BAG2 vectors (F) for 24 h prior to H37Ra infection. Cell apoptosis and viability was measured separately by western blot and Cell Titer-Glo assays. (G and H) RAW264.7 cells and BMDMs were transfected with control siRNA or *Bag2* siRNA, and then infected with H37Ra. Bacterial viability was detected by CFU assays (G). Detached cells found in the supernatants were counted; viability was assessed by trypan blue exclusion. The results are expressed as percentage of the cells compared to the total number of cells in the sample (H). The data are representative of 3 independent experiments. Results represent means ± SD. *p < 0.05, relative to the uninfected control.

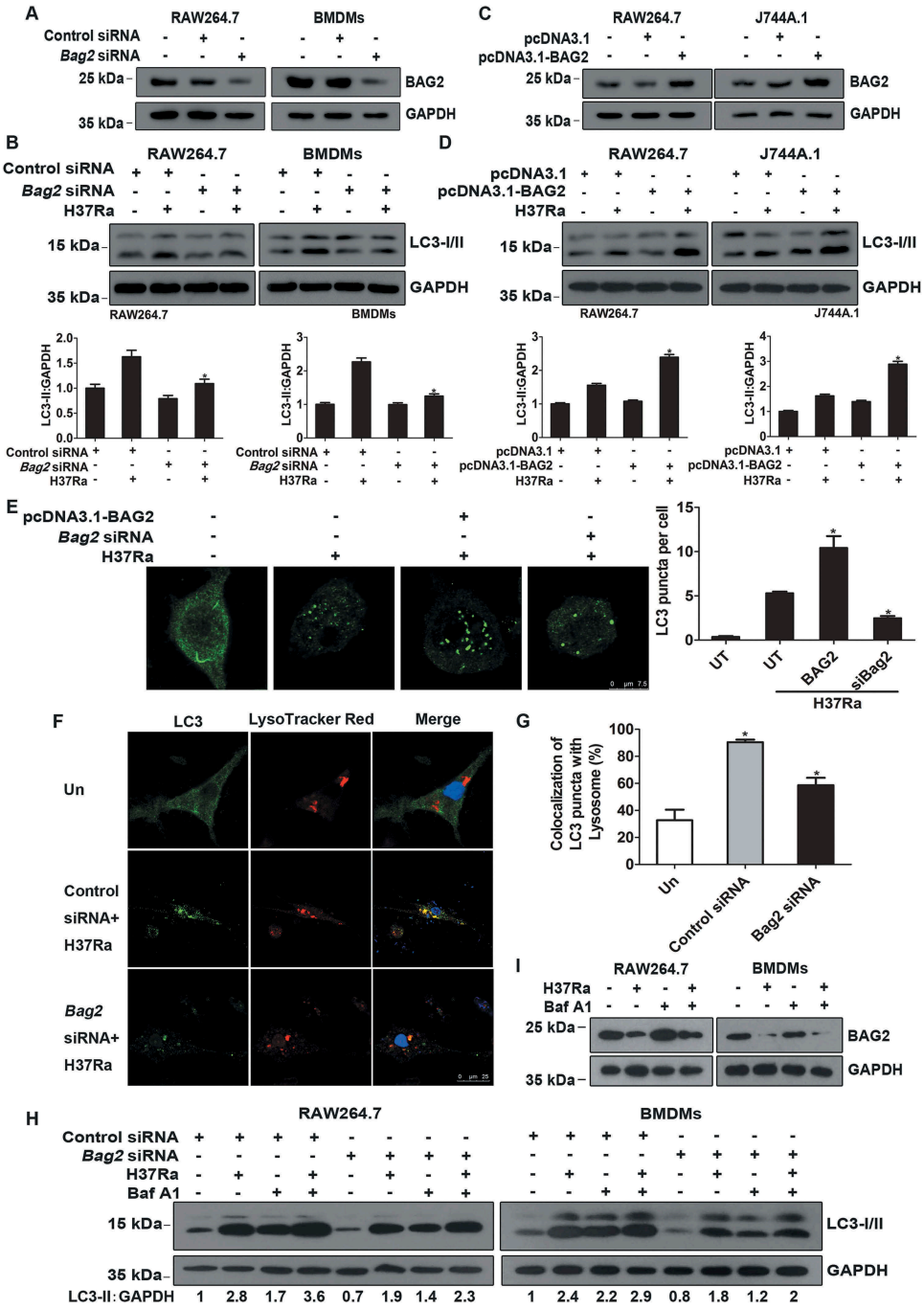

Figure 2. BAG2 promotes autophagy during *M. tuberculosis* infection. (A) RAW264.7 cells and BMDMs were transfected with control siRNA or *Bag2* siRNA. BAG2 protein levels were determined by western blot. (B) RAW264.7 cells and BMDMs were transfected with control siRNA or *Bag2* siRNA following H37Ra infection or not. Upper panel: representative LC3 protein levels images of 3 independent replicates are shown. Lower panel: quantitative analysis of the LC3-II band normalized to GAPDH is shown. (C) RAW264.7 and J744A.1 cells were transfected with empty vector or BAG2 expression vector. BAG2 protein levels were determined by western blot. (D) RAW264.7 and J744A.1 cells were transfected with empty vector or BAG2 expression vector followed by H37Ra infection or not. Expression of LC3 was analyzed by western blot. Lower panel: quantitative analysis of the LC3-II band normalized to GAPDH is shown. (E) RAW264.7 cells were transfected with empty vector, BAG2 expression vector, or *Bag2* siRNA and then either infected or not with H37Ra followed by anti-LC3 antibody staining. The LC3 puncta were detected by confocal microscopy. Quantitative analysis of LC3 puncta formation (right) is shown. Scale bar: 7.5 μm. (F) RAW264.7 cells transfected with control siRNA or *Bag2* siRNA were infected with H37Ra or not. The cells then were stained with LysoTracker to detect lysosomes (red) and immunolabeled with anti-LC3 antibody (green). Representative immunofluorescence images of 3 independent replicates are shown. Scale bar: 25 μm. (G) The percentage of colocalization of LC3 puncta and lysosomes. (H) RAW264.7 cells and BMDMs transfected with control siRNA or *Bag2* siRNA were infected, with or without Baf A1 pretreatment. LC3 expression was detected by western blot. (I) RAW264.7 cells and BMDMs were pretreated without or with Baf A1 and then uninfected or infected with H37Ra. BAG2 expression was discerned by western blot. Results represent means ± SD (n = 3). *p < 0.05 vs. the control group. Un, untreated.

that the function in BAG2 is related to SQSTM1. Next, specific domains of SQSTM1 and BAG2 of importance for the relationship were studied in RAW264.7 cells. SQSTM1 protein contains an N-terminal PB1 domain [29], a C-terminal UBA domain [30] and a middle region LIR [31]. To define the regions of SQSTM1 required for the

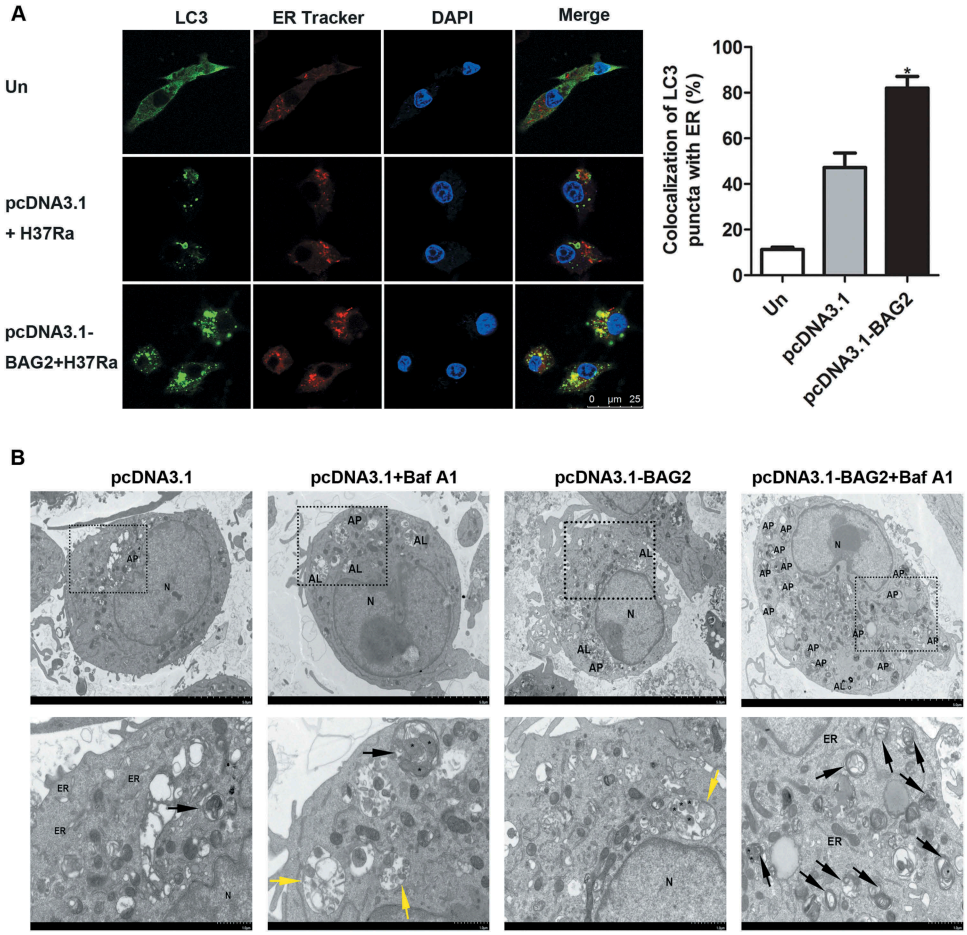

Figure 3. BAG2 induces reticulophagy in macrophages during *M. tuberculosis* infection. (A) RAW264.7 cells were transfected with empty vector or BAG2 expression vector, and then infected with H37Ra. Reticulophagy were determined by assessing the colocalization between LC3-positive autophagosomes (green) and ER Tracker labeled endoplasmic reticulum (red). The percentage of colocalization of LC3 puncta and ER is shown (right). Scale bar: 25 μm. (B) RAW264.7 cells were transfected with the control or BAG2 vector, then treated with H37Ra infection and Baf A1 pretreatment or not. Electron microscopy images showing ultrastructures of cells. Black arrows point to autophagosomes (AP). Yellow arrows point to autolysosome (AL). Asterisks indicates ER fragments inside AP. Lower panels show enlarged insets. N, nucleus. Data are shown as the mean ± SD of 3 independent experiments. *$p < 0.05$. Un, untreated.

BAG2-SQSTM1 interaction, the different truncated SQSTM1 vectors with HA-tag and BAG2-FLAG expression vectors were co-transfected into RAW264.7 cells. Results of co-IP assays showed that the interaction between BAG2 and SQSTM1 is mainly dependent on PB1 and UBA domains of SQSTM1 (Figure 4B and C). The results were corroborated further by immune-colocalization assays (Figure 4A). On the other hand, the regions of BAG2 required for the BAG2-SQSTM1 interaction was examined by co-transfecting cells with different FLAG-tagged BAG2 deletion mutant constructs and SQSTM1-HA expression vectors followed by co-IP assays. BAG2 contains a C-terminal BAG domain (amino acids 109–189) [32]. The fragments containing the BAG domain interacted with SQSTM1 (Figure 4D and E). These results showed that PB1 and UBA domains of SQSTM1 and BAG domain of BAG2 are essential for the BAG2-SQSTM1 interaction.

To examine whether the interaction between SQSTM1 and BAG2 is involved in regulating reticulophagy, RAW264.7 cells transiently expressing pcDNA3.1 or pcDNA3.1-BAG2 were infected. Fluorescence images showed that SQSTM1 localized to the ER fraction and BAG2 overexpression increased colocalization of SQSTM1 and ER in infected RAW264.7 cells (Figure 5A). To further investigate the effect of interaction between BAG2 and SQSTM1 on the recruitment of SQSTM1 to ER, we transfected RAW264.7 cells with pcDNA3.1-BAG2 B2 (deletion of the BAG domain). Compared with RAW264.7 cells overexpressing BAG2, the quantity of ER-localized SQSTM1 was decreased in cells expressing the SQSTM1 binding-defective pcDNA3.1-BAG2 B2 (Figure 5A). Additionally, we also observed that BAG2 overexpression did not increase colocalization of FAU (Figure 5B), a precursor of antimicrobial polypeptide [33] or ubiquitinated proteins (Figure 5C) with *M. tuberculosis* H37Ra phagosomes in RAW264.7 cells, suggesting that SQSTM1 are prone to target to ER in BAG2-overexpressed macrophages during infection. Collectively, these data indicated that BAG2 is

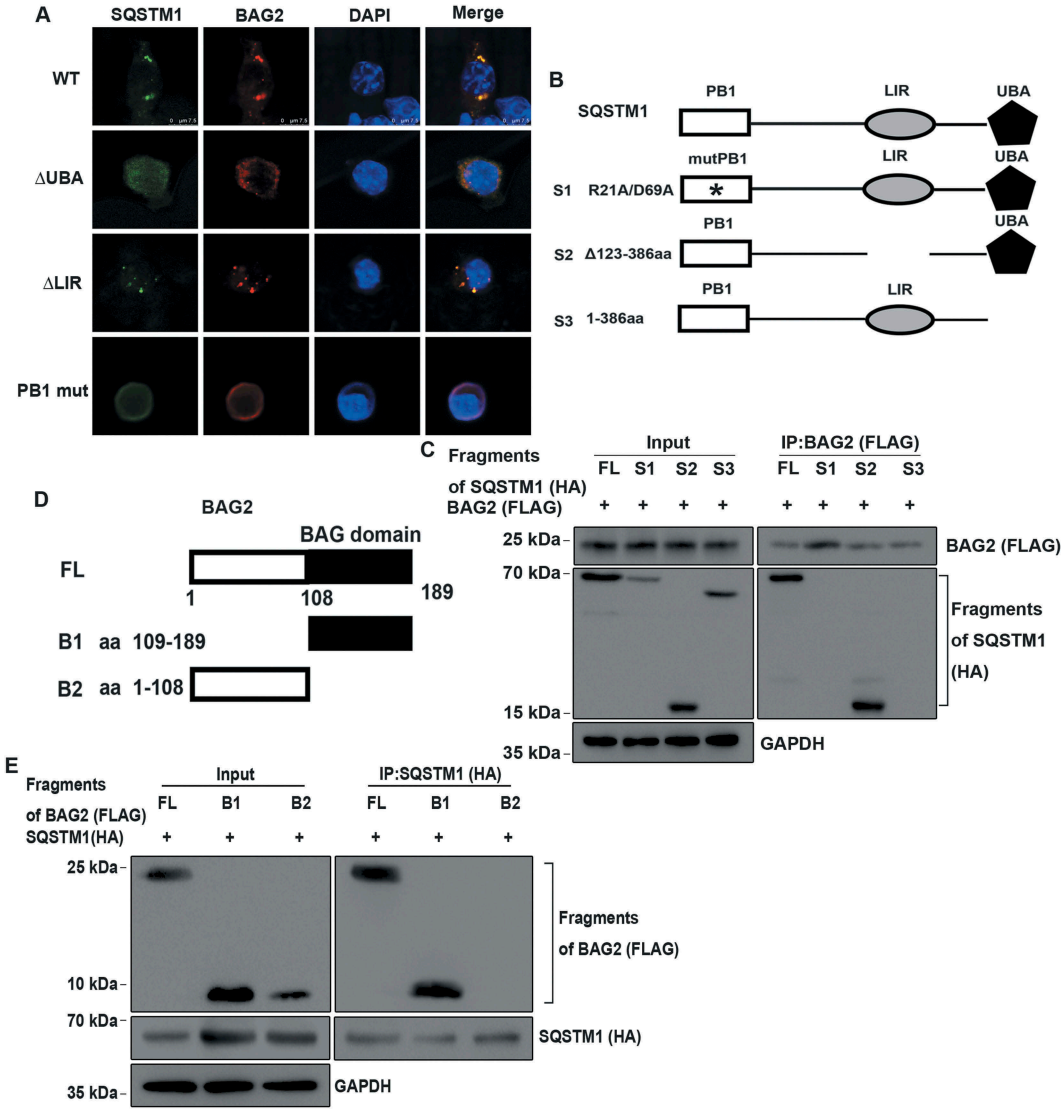

Figure 4. BAG2 interacts with SQSTM1 in RAW264.7 cells. (A–C) RAW264.7 cells were co-transfected expression vectors of HA-tagged SQSTM1 fragments with BAG2-Flag expression vectors. (A) The transfected cells were microscopically analyzed for colocalization of BAG2 and SQSTM1. Scale bar: 7.5 μm. (B) Schematic diagram showing the domain structure of SQSTM1. (C) The cell lysates were immunoprecipitated by FLAG. Protein expression levels were assayed by western blot. (D and E) RAW264.7 cells were co-transfected expression vectors of BAG2-FLAG fragments with SQSTM1-HA expression vectors. (D) Schematic diagram showing the BAG2 domain structure. (E) The interaction was assessed using co-IP as indicated.

required for the recruitment of SQSTM1 into ER and removed excess ER in infected macrophages.

BAG2 protects macrophages from ER stress-induced apoptosis by promoting autophagy during M. tuberculosis *infection*

To assess the role of autophagy in modulating cell death induced by *M. tuberculosis* H37Ra, BMDMs and RAW264.7 cells were pre-treated respectively with Baf A1, an inhibitor of autophagic vacuole and lysosome fusion, and 3-methyladenine (3-MA), a known inhibitor of autophagy, prior to infection. These treatments rendered macrophages more sensitive to killing by H37Ra (Figure 6A–D), indicating that autophagy contributes to the survival of H37Ra-infected cells. Consistently, knockdown of the autophagy protein ATG5 also increased further macrophages apoptosis induced by H37Ra (Figure 6E–G).

To determine whether apoptosis is attenuated by BAG2-induced autophagic flux activation, BAG2 was overexpressed with or without Baf A1 in H37Ra-infected macrophages. Inhibition of autophagy partially abolished the protective capability of BAG2 in cell survival (Figure 6H). Simultaneously, knockdown of *Bag2* did not further increase cell apoptosis induced by *M. tuberculosis* H37Ra when autophagy was inhibited (Figure 6I). Taken together, these findings indicated that

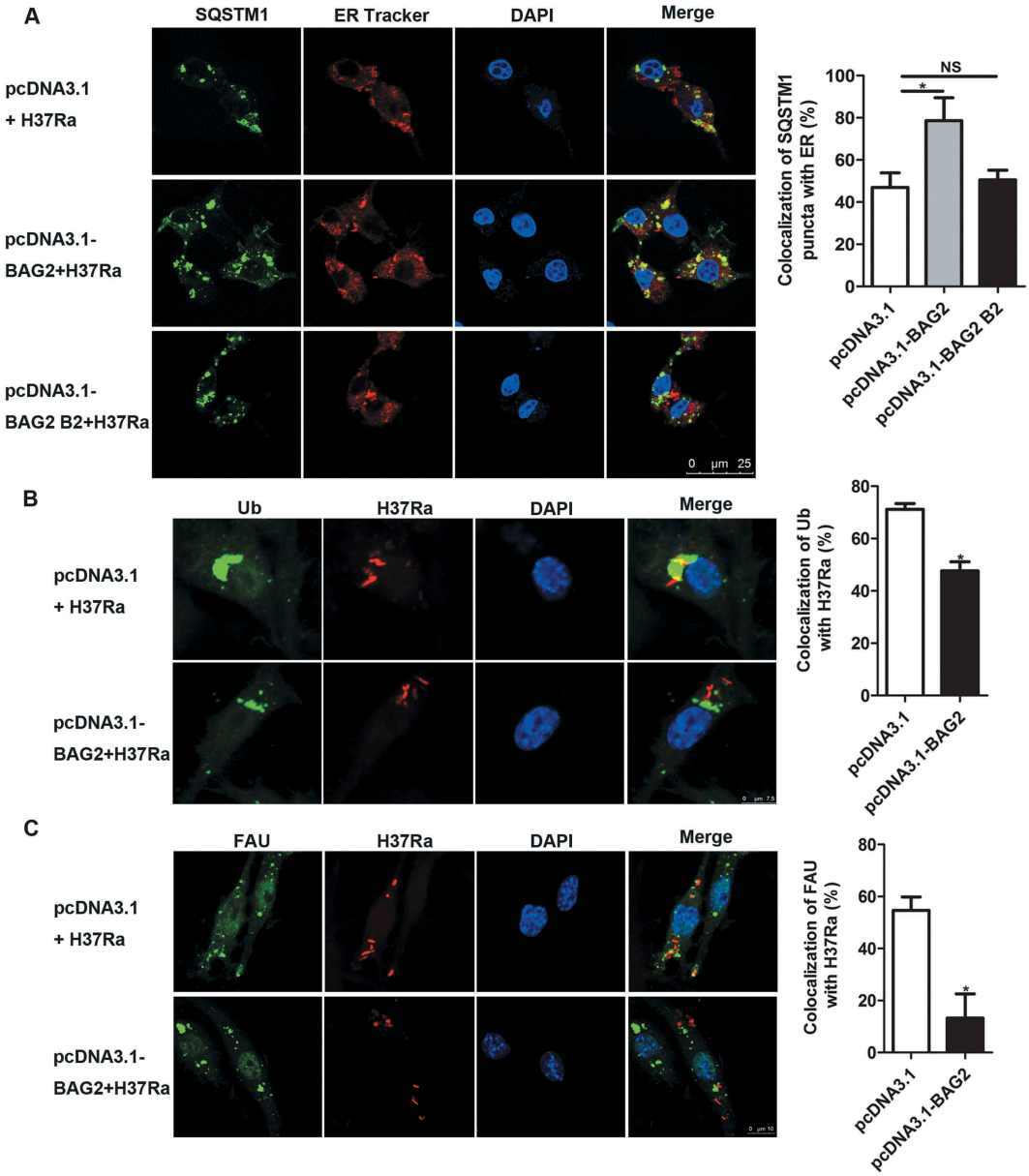

Figure 5. SQSTM1 was required for BAG2-enhanced reticulophagy during *M. tuberculosis* infection. (A) RAW264.7 cells were transfected with empty vector, BAG2 expression vector or BAG2 B2 and then infected with H37Ra. Colocalization between SQSTM1 (green) and ER Tracker-labeled endoplasmic reticulum (red) was visualized by immunofluorescence. The percentage of colocalization of SQSTM1 and ER is shown (right). Scale bar: 25 μm. (B) RAW264.7 cells were transfected with empty vector or BAG2 expression vector, then infected with Texas Red-labeled H37Ra. Cells were fixed and stained for ubiquitin conjugates. The percentage of colocalization of ubiquitin conjugates and H37Ra are shown (right). Scale bar: 7.5 μm. (C) RAW264.7 cells were transfected with empty vector or BAG2 expression vector, then infected with Texas Red-labeled H37Ra. Cells were fixed and stained for FAU. The percentage of colocalization of FAU and H37Ra are shown (right). Scale bar: 10 μm. Data represent mean ± SD from at least 3 independent experiments.

BAG2 promotes macrophage survival upon ER stress induced by *M. tuberculosis* H37Ra through activation of autophagy.

BAG2 promotes BCL2-BECN1 complex disassociation in M. tuberculosis *H37Ra-infected RAW264.7 cells*

Autophagy is triggered when the BECN1-BCL2 interaction is disrupted [34,35]. The antiapoptotic BCL2 family regulates BECN1-dependent autophagy [36–38]. To investigate the effect of BAG2 on the interaction between BCL2 and BECN1, we performed co-IP of RAW264.7 cells with transiently transfected with *Bag2* siRNA during infection. Knockdown of *Bag2*, and the addition of the MAPK/ERK inhibitor U0126 inhibited the disassociation of BCL2 and BECN1 in *M. tuberculosis* H37Ra–infected RAW264.7 cells (Figure 7A). Indeed, knockdown of *Bag2* inhibited phosphorylation of MAPK1/3 and BCL2 during infection (Figure 7B), indicating that BAG2 regulated interaction between BCL2 and BECN1 through MAPK1/3-mediated phosphorylation of BCL2. Afterward, endogenous BAG2 interacted with BCL2 as demonstrated via

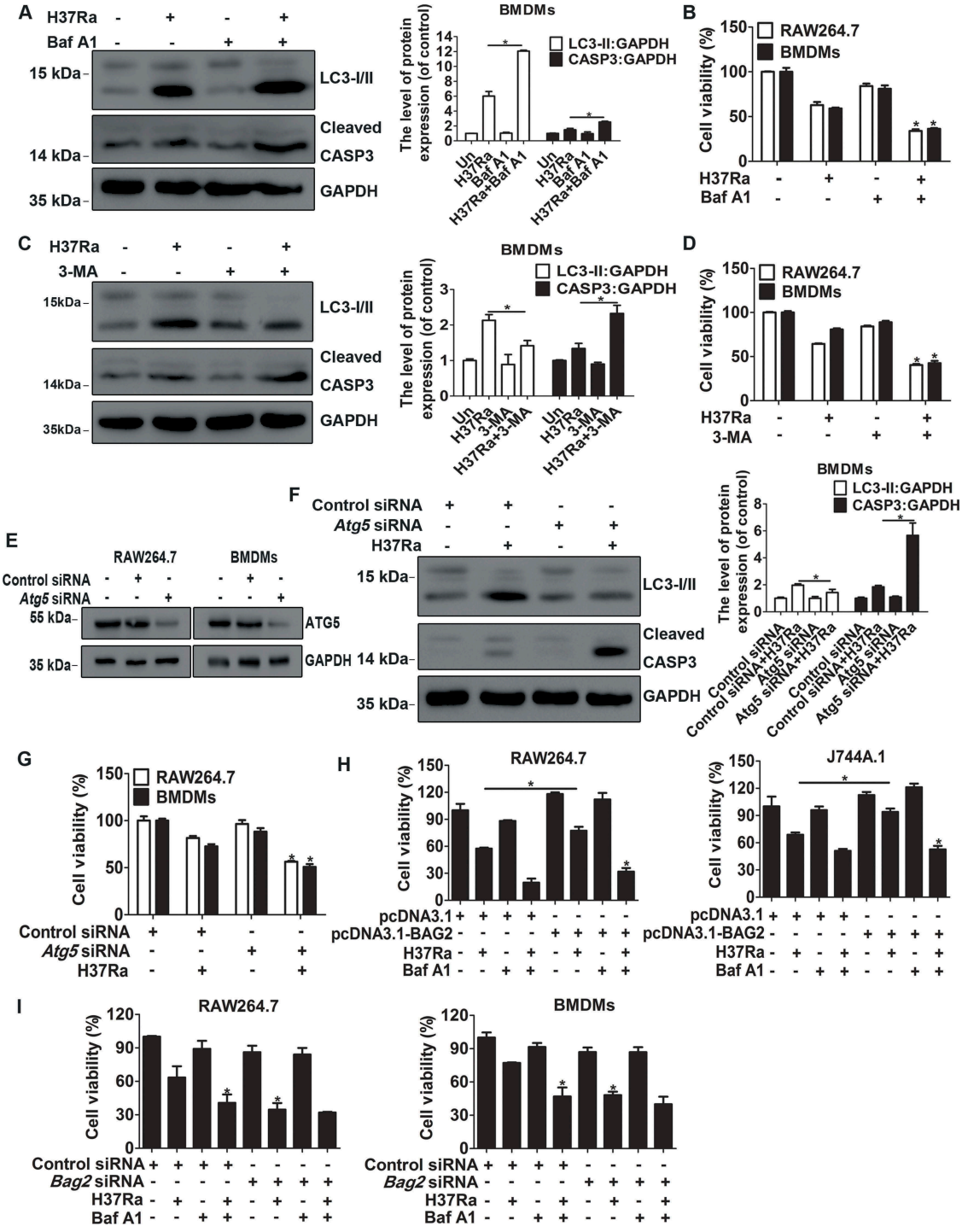

Figure 6. BAG2 inhibits H37Ra-induced apoptosis in macrophages. (A–D) RAW264.7 cells and BMDMs were pre-treated with bafilomycin A_1 (Baf A1) (100 nM) (A and B) or 3-methyladenine (3-MA) (10 μM) (C and D) for 2 h, and then were uninfected or infected with H37Ra. Cell apoptosis and viability was measured separately by western blot (A and C) and Cell Titer-Glo assays (B and D). (E) RAW264.7 cells and BMDMs were transfected with control siRNA or *Atg5* siRNA. ATG5 expression was detected using western blot. (F and G) RAW264.7 cells and BMDMs were transfected with control siRNA or *Atg5* siRNA and then infected without or with H37Ra. Cell apoptosis and viability was tested respectively using western blot (F) and Cell Titer-Glo assays (G). (H and I) RAW264.7 and J744A.1 cells transfected with empty vector or BAG2 expression vector (H), or RAW264.7 cells and BMDMs transfected with control siRNA or *Bag2* siRNA (I) were infected, with or without Baf A1 pre-treatment. Cell viability was determined using Cell Titer-Glo assays. Results represent means ± SD (n = 3). *p < 0.05 vs. the control group.

co-IP assays in RAW264.7 cells (Figure 7C). Knockdown of *Bcl2* resulted in dissociation BAG2 and BECN1 in RAW264.7 cells (Figure 7D), implicating that the interaction between BAG2 and BECN1 relies on BCL2. These

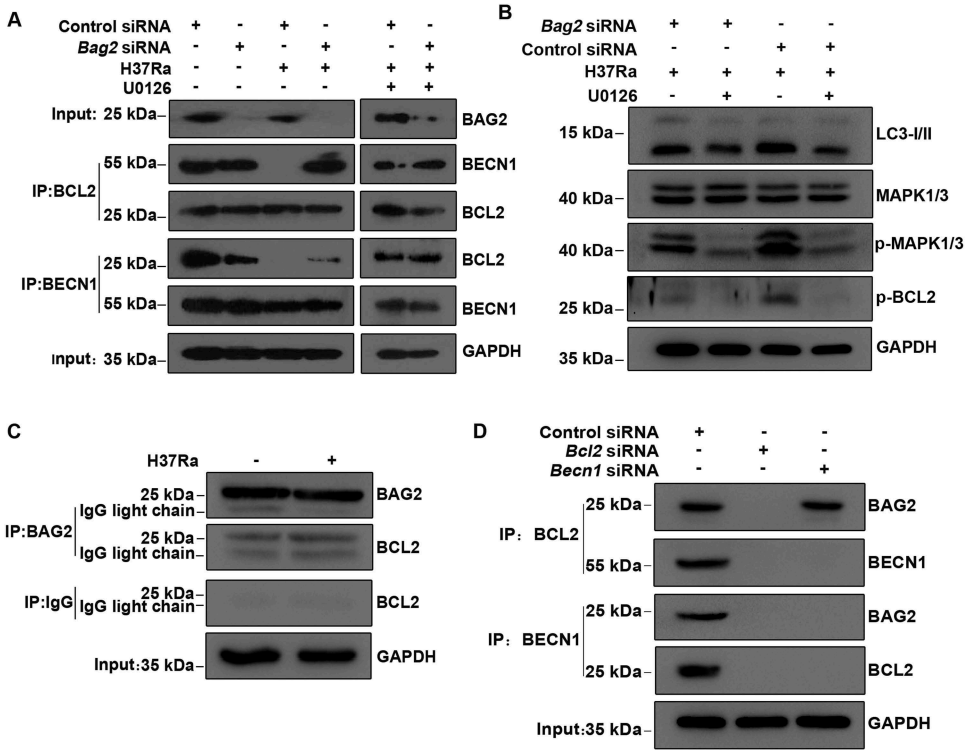

Figure 7. BAG2 promotes disassociation of the BCL2-BECN1 complex in *M. tuberculosis* H37Ra-infected RAW264.7 cells. (A and B) RAW264.7 cells were transfected with control or *Bag2* siRNA and then either infected or not with H37Ra as well as either pre-treated with or without U0126 (10 μM) for 2 h. The cell lysates were immunoprecipitated by BCL2 or BECN1(A). Protein expression levels were assayed by western blot (A and B). (C) RAW264.7 cells were uninfected or infected with H37Ra. The cell lysates were immunoprecipitated by BAG2. Immune complexes were analyzed by western blot. (D) RAW264.7 cells were transfected with control siRNA, *Bcl2* siRNA, or *Becn1* siRNA. Cell lysates were assayed via co-IP, and protein levels were determined by immunoblotting. All results are representative of 3 independent experiments.

results demonstrated that BAG2 disrupts the association between BECN1 and BCL2 to trigger autophagy in *M. tuberculosis* H37Ra-infected RAW264.7 cells.

XBP1 is required for downregulation of BAG2 expression during M. tuberculosis *H37Ra-induced ER stress*

To identify the UPR signaling pathway responsible for inhibition of BAG2 expression in macrophages under H37Ra-induced ER stress, we interfere with the expression of 3 ER sensors, ATF6, EIF2AK3 or ERN1 in BMDMs and RAW264.7 cells (Figure 8A) [39]. As shown in Figure 8B, knockdown of *Ern1* recovered BAG2 expression and increased autophagy flux in H37Ra-infected BMDMs and RAW264.7 cells. Thus, the ERN1 branch of the UPR is responsible for downregulation of BAG2 during infection.

XBP1 is downstream of ERN1 in the UPR pathway [40,41]. Thus, we investigated whether XBP1 contributes to BAG2 downregulation in infected BMDMs and RAW264.7 cells via knockdown of *Xbp1* (Figure 8C). Silence of the XBP1 protein restored BAG2 expression, and rescued BAG2 decrease-mediated autophagy inhibition in infected macrophages (Figure 8D and E).

To investigate the promoter region of *Bag2* in response to H37Ra-induced ER stress, a series of progressively truncated luciferase reporter constructs (pGL4.10-BAG2-) (positions −1892 to +19) were transiently transfected into RAW264.7 and J744A.1 cells. We found that deletion of the region between −321 and +19 resulted in a substantial decrease in promoter activity, and H37Ra no longer inhibited transcriptional activity of *Bag2* (Figure 8F and G). The minimal promoter that was responsive to ER stress was the region between −586 and +19 (Figure 8F and G). Therefore, the region between −586 and −321 is essential for the H37Ra-mediated change in *Bag2* transcription in macrophages.

To determine if transcription factor XBP1 binds to the *Bag2* promoter, we performed chromatin immunoprecipitation (ChIP) assays in RAW264.7 and J744A.1 cells during infection. The *Bag2* upstream region was tested by 9 different pairs of primers, which divided the *Bag2* promoter region into 9 fragments. An XBP1-specific binding site was identified at fragment 8 (Figure 8H). Consistent with the luciferase reporter assay results, the binding site was located in the −586 to −321 region of the promoter. Collectively, these studies demonstrated that XBP1 binds to the *Bag2* promoter and transcriptionally inhibits BAG2 expression during *M. tuberculosis* H37Ra-induced ER stress.

Discussion

In this study, we demonstrated that BAG2 contributes to survival of murine macrophages undergoing ER stress induced by *M. tuberculosis* through activating selective autophagy.

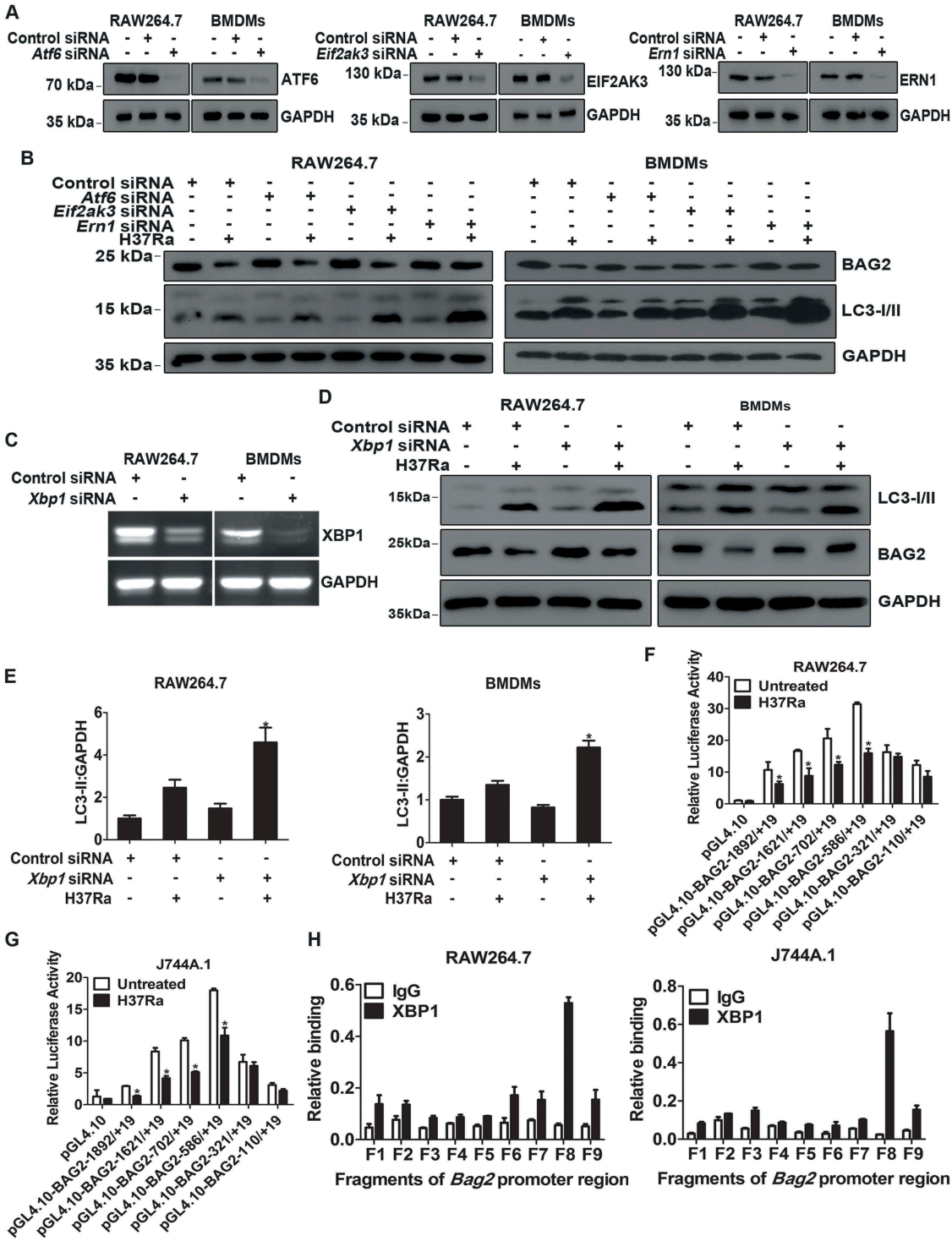

Figure 8. XBP1 is responsible for transcriptional inhibition of *Bag2* during *M. tuberculosis* H37Ra-induced ER stress. (A) RAW264.7 cells and BMDMs were transfected with control siRNA, *Atf6* siRNA, *Eif2ak3* siRNA, or *Ern1* siRNA. ATF6, EIF2AK3 and ERN1 protein levels were detected by western blot. (B) RAW264.7 cells and BMDMs transfected with control siRNA, *Atf6* siRNA, *Eif2ak3* siRNA or *Ern1* siRNA remained uninfected or were infected by H37Ra, and then BAG2 and LC3 protein levels were detected by western blot. (**C**) RAW264.7 cells and BMDMs were transfected with control siRNA or *Xbp1* siRNA. The expression levels of *Xbp1* mRNA were detected by RT-PCR. (D and E) RAW264.7 cells and BMDMs were transfected with control siRNA or *Xbp1* siRNA and then infected with H37Ra. (D) Western blot was performed to test BAG2 and LC3 levels. (E) Quantitative data of LC3-II was shown. (F and G) Before infection with H37Ra, *Bag2* promoters of different lengths were transfected into RAW264.7 (F) and J744A.1 cells (G) for 48 h. The relative luciferase activity was calculated as fold change relative to the empty pGL4.10 vector. (H) ChIP assays were performed in infected RAW264.7 and J744A.1 cells using antibodies directed against XBP1 or IgG control. After immunoprecipitation, DNA was amplified by qPCR using specific primers for the *Bag2* promoter region. Data are shown relative to qPCR using input DNA before immunoprecipitation. Data are mean ± SD of 3 separate experiments, *$p < 0.05$.

During *M. tuberculosis*-induced ER stress, expression of endogenous BAG2 was reduced, and cells were relatively sensitive to apoptosis. Similarly, overexpression of BAG2 promoted autophagy activation and rendered macrophages relatively resistant to *M. tuberculosis*-induced apoptosis. Conversely, knockdown of *Bag2* limited autophagy in response to *M. tuberculosis* and increased cell apoptosis. Moreover, we showed that the effect of BAG2 on autophagy was through phosphorylation of BCL2, which was modulated by MAPK/ERK, and blocked the interaction between BECN1 and BCL2. Additionally, *M. tuberculosis*-mediated BAG2 downregulation was caused by a transcriptional inhibition of the ERN1-XBP1 axis of the UPR.

Our research and previous studies [42] showed that *M. tuberculosis* infection induces the ER stress-signaling pathway. This was confirmed by UPR markers [43,44], particularly, HSPA5 and DDIT3 expression increased during mycobacterial infection. ER stress as a result of misfolded protein accumulation can lead to cell apoptosis [45,46] and is simultaneously a pathway to induce autophagy [47,48]. We observed that autophagy inhibition led to enhance *M. tuberculosis*-induced apoptosis, indicating mild autophagy could protect cells from such apoptosis. In this study, BAG2 promoted autophagy, thereby decreasing cell death, whereas inhibition of autophagy abolished BAG2-mediated cytoprotection during *M. tuberculosis* infection. These results elucidated the relationship of autophagy and apoptosis and the role of BAG2 in *M. tuberculosis*-induced ER stress.

Our results demonstrated that BAG2 promotes autophagy, and we explored the mechanism by which this phenomenon occurs. Recently, it was reported that the interaction between anti-apoptotic protein BCL2 and the autophagy protein BECN1 plays a critical role in apoptotic and autophagic machineries [49,50]. Therefore, we investigated the effect of BAG2 on the dissociation of BECN1 from BCL2, and we found that BAG2 limits BECN1-BCL2 complex formation by phosphorylating BCL2 during *M. tuberculosis* infection. BCL2 participates in the regulation of cell death and survival during apoptosis and autophagy [51,52]. Phosphorylation of BCL2, by kinases of the JNK or MEK signaling pathways, contributes to anti-apoptotic activity [53] and autophagic activation [54,55]. Our results indicated that BAG2 is involved in regulating BCL2 phosphorylation through the MAPK/ERK pathway, because inhibition of BAG2 suppressed the activation of MAPK1/ERK2-MAPK3/ERK1 and BCL2 during mycobacterial infection.

Reticulophagy has been recognized as an effective and targeted way to remove damaged ER and ensure cell survival under live Gram-positive bacteria caused-ER stress [10]. Several proteins have also been reported as signaling molecules, including RETREG1/FAM134B [48], CCPG1 [56] and SEC62 [57]. In our study, double-labeled immunofluorescence and transmission electron microscopy analysis suggested that BAG2 increased the localization of LC3 and autophagosome in the ER (reticulophagy) during *M. tuberculosis* infection. In contrast to RETREG1, BAG2 does not have a LIR motif and reticulon domain that can be associated with the ER membrane. Its function on the reticulophagy is likely a secondary effect. Of note, SQSTM1 could recruit LC3-II-positive autophagosomes to the ubiquitin-SQSTM1-decorated ER to initiate reticulophagy [28] and SQSTM1 also interacted with BAG2. The finding that there was increased LC3 and SQSTM1 in ER after BAG2 overexpression during *M. tuberculosis* infection might support this notion, which BAG2 promoted reticulophagy by recruitment of SQSTM1 in ER. Meanwhile, the results that BAG2 decreased colocalization of ubiquitinated proteins or FAU and *M. tuberculosis* phagosomes also further indicated that BAG2 could render SQSTM1 relatively prone to locate in ER, thereby decreasing delivery of specific ribosomal and bulk ubiquitinated cytosolic proteins to mycobacterial phagosomes by SQSTM1 [33]. However, the molecules mechanism of this recruitment process remains to be determined.

When ER stress is induced, cells trigger the UPR causing the activation of the ERN1, ATF6 and EIF2AK3 pathways [58]. We observed that *Ern1* knockdown recovered BAG2 expression during *M. tuberculosis* infection, suggesting that ERN1 pathway is responsible for downregulation of BAG2. Upon activation, ERN1 initiates an unconventional splicing of *Xbp1* mRNA, producing a functional isoform that encodes the transcription factor [59,60]. We identified XBP1 as the transcription factor, which was responsible for *M. tuberculosis*-mediated transcriptional downregulation of *Bag2*. This was confirmed in macrophages by knockdown of *Xbp1*, which blocked the inhibition of *M. tuberculosis* in expression of BAG2, and ChIP data also demonstrated that XBP1 bound to the *Bag2* promoter.

Studies with RNA interference confirmed that knockdown of *Ern1*/*Xbp1* triggered autophagy. Compared to our results, different studies exhibited that ER stress activates autophagy through UPR stress sensors *in vitro* [61–63]. However, of the known XBP1 deficiency can also trigger EIF2AK3-dependent autophagy as a feedback loop in an attempt to provide cellular protection [64,65], and in our study, ER stress did not activate autophagy at late stage during infection. Moreover, our results also showed that knockdown of *Xbp1* contribute to autophagy-mediated cytoprotection by restoring BAG2 expression during *M. tuberculosis*-induced ER stress, suggesting that prolonged or excessive ER stress could utilize XBP1 to inhibit BAG2-induced autophagy, thereby exacerbating cell apoptosis at the late stage of infection.

In summary, our data provided sufficient evidence that BAG2 inhibits ER stress-induced apoptosis upon *M. tuberculosis* infection through activation of autophagy, which was mediated by disassociation of BCL2 from BECN1 as a result of MAPK/ERK-mediated phosphorylation of BCL2. BAG2 contributes to reticulophagy by recruitment of SQSTM1. Moreover, we showed that XBP1 of the ERN1 pathway is a novel transcriptional suppressor of *Bag2* and alleviates autophagy of macrophages. Therefore, BAG2 appears to be a part of the host defense mechanism in *M. tuberculosis*-infected macrophages by acting as a critical role of a signaling pathway of ERN1-XBP1-BAG2-MAPK1/3-BECN1-autophagy. Our results contribute to further understanding of the regulatory mechanisms of intracellular homeostasis in defending bacterial infection.

Materials and methods

Animal experiments

Female C57BL/6 mice (6–8 weeks old) were purchased from the Laboratory Animal Center of the Fourth Military Medical

University (Xi'an, Shaanxi, China). All animal experiments were performed according to the Guidelines for the Care and Use of Animals of Northwest A&F University (Yangling, China).

Cell and bacterial cultures

Mouse bone marrow-derived macrophages (BMDMs) were isolated from C57BL/6 mice and maintained in RPMI1640 media (Gibco, 31800–022) supplemented with 10% fetal bovine serum (Gibco, 10099–141), 100 IU/mL penicillin and 100 μg/mL streptomycin (Beyotime, ST488), and 50 ng/mL M-CSF/macrophage colony-stimulating factor (R&D Systems, 416-ML-010). The murine macrophage cell lines RAW264.7 (ATCC, TIB71) and J774A.1 (ATCC, TIB67) were cultured in RPMI1640 media containing 10% fetal bovine serum. All cells were incubated in a 37°C humidified incubator with 5% CO_2. *M. tuberculosis* H37Rv (kindly provided by Zhigang Song, Shanghai Public Health Clinical Center, China) and H37Ra (ATCC 25177) strains were cultured in Middlebrook 7H9 broth medium (Sigma-Aldrich, M0178) or 7H10 agar plates (Sigma-Aldrich, M0428) supplemented with 10% OADC (Sigma-Aldrich, M0678).

Infection and colony forming unit (CFU) assays

Cells were infected with *M. tuberculosis* at a multiplicity of infection of 1:10 for 4–6 h. Then, the cells were washed 3 times with PBS (Gibco, 10010–023) to remove extracellular bacteria. The infected cells were cultured for 24 h. Thereafter, intracellular bacteria were harvested and plated on 7H10 agar plates supplemented with 10% OADC. After 3–4 weeks of culture, values were expressed as CFU:well.

Transient transfections and chemical treatment

All plasmid and siRNA (GenePharma, Shanghai, China) transfections were performed using Lipofectamine 3000 (Invitrogen, L3000-015) according to the manufacturer's protocol.

Various chemical reagents were used to pre-treat macrophages: (a) bafilomycin A_1 (Baf A1, 100 nM; Selleck, S1413) and 3-methyladenine (3-MA, 10 μM; Sigma-Aldrich, M9281) to inhibit autophagy; (b) U0126 (10 μM; Sigma-Aldrich, 19–147) to inhibit the MAPK/ERK pathway. All the above treatments were applied 2 h before bacterial stimulation and maintained until the end of the experiments. Tunicamycin (TM, 10 μg/mL; Sigma-Aldrich, T7765) and thapsigargin (TG, 0.5 μM; Sigma-Aldrich, T9033) were used to induce ER stress.

Cell viability assays

Cell viability was determined using the luminescent cell viability assay kit (Promega, G7571), according to the manufacturer's protocol. Briefly, cells were seeded in each well of a 96-well plate for 24 h at 37°C and performed the desired treatment afterward. Then, cells were incubated with the CellTiter-Glo® Reagent at room temperature. Luminescent signal of each sample was detected using a microplate reader (PerkinElmer, Cetus, Norwalk).

Chromatin immunoprecipitation (ChIP) analysis

Macrophages were prepared for chromatin immunoprecipitation (ChIP) assays using the ChIP assay kit (Cell Signaling Technology, 9005) according to the manufacturer's protocol. XBP1 primary antibodies (Santa Cruz Biotechnology, sc-8015) or IgG (Beyotime, A7028) were used. Purified DNA was used as qPCR template to detect the presence of the *Bag2* promoter. The primers used to detect DNA fragments are shown in Table S1.

Promoter reporter construct and dual-luciferase reporter assays

The *Bag2* promoter sequence was analyzed using Ensembl and NCBI. Six progressive truncated fragments containing from −1892 to +19 relative to the transcription initiation site were cloned into the luciferase reporter vector pGL4.10 (Promega, E665A). Primer sequences for promoter reporter plasmid construction are listed in Table S2. Macrophages were co-transfected with luciferase constructs and the pRL-TK vector (Promega, E2241). The cells were harvested 36–48 h after transfection and were detected using the dual-luciferase reporter assay system (Promega, E1910).

Co-immunoprecipitation (co-IP) assay

Cells were lysed using IP lysis buffer (Thermo Scientific, 87787) with protease inhibitors (Gibco, A32955) on ice. Whole cell lysates were incubated with 2 μg primary antibody and rotated overnight at 4°C. Then, 20 μL Protein A/G plus agarose (Thermo Scientific, 20423) were added to pull down immune complexes for 2 h at 4°C on an orbital shaker. Beads were washed 3 times with ice-cold wash buffer and then eluted by boiling in loading buffer. Complexes were detected via western blot.

Immunofluorescence and confocal microscopy

After the relevant treatment, cells on coverslips were washed with PBS, fixed with 4% paraformaldehyde in PBS for 15 min, permeabilized, and blocked with 10% BSA (Beyotime, ST023) for 2 h at room temperature. Cells were incubated with primary antibody overnight at 4°C and, then, with a fluorescently labeled secondary antibody for 2 h at room temperature. In some experiments, RAW264.7 cells were loaded with LysoTracker and ER Tracker (Invitrogen, E34250), or DAPI (Sigma-Aldrich, D9542) for the indicated time periods, and then washed 3 times with PBS before fixation for immunostaining. After mounting, the stained cells were visualized with a confocal microscope (Leica Microsystems GmbH, Wetzlar, Germany). To quantitate autophagy and colocalization, we analyzed the cells using

Image-Pro Plus analysis software. Each condition was assayed in triplicate, and at least 100 cells per well were counted.

Reverse transcription PCR and quantitative PCR (qPCR)

Total RNA was isolated using the Trizol reagent (Invitrogen, 93289) according to the manufacturer's instructions. RNA was reverse transcribed using a PrimeScript RT Reagent Kit (TaKaRa, RR037A). qPCR was carried out using the ABI StepOnePlus PCR system (Applied Biosystems, Foster City, CA, USA) using the TB Green Premix Ex Taq II (TaKaRa, RR82LR) with specific primers (Table S1). The $2^{-\Delta\Delta Ct}$ method was used to determine the relative changes in gene expression normalized to *Gapdh*.

Western blotting

Proteins were isolated using RIPA buffer (Pierce, Rockford, IL, USA), according to the manufacturer's instructions. Protein extracts were separated by SDS-PAGE and then transferred to PVDF membranes (Millipore, ISEQ00010) and incubated with appropriate antibodies. Anti-BAG2 (ab80596), anti-FAU (ab81442) and anti-BECN1 (ab62557) were from Abcam. Anti-HA-tag (3724), anti-Cleaved CASP3 (9661), anti-SQSTM1 (23214), anti-DDIT3 (5554), anti-HSPA5 (3177), anti-ATG5 (12994), anti-BCL2 (3498), anti-p-BCL2 (2827), anti-MAPK3/1 (ERK1/2; 4695), anti-p-MAPK3/1 (p-ERK1/2; 4370) and anti-ATF6 (65880) were purchased from Cell Signaling Technology. Anti-LC3B (BL8918) and anti-FLAG (F1804) were from Sigma-Aldrich. Anti-mono and polyubiquitin conjugates (FK2; BML-PW8810-0100) was from Biomol. Anti-ERN1 (sc-390960) and anti-EIF2AK3 (sc-377400) were from Santa Cruz Biotechnology. Anti-GAPDH (HC301) was from TransGen Biotech Co. Secondary antibodies (A0208 and A0216) were purchased from Beyotime. Proteins were visualized using the SuperSignal West Pico Substrate (Thermo Fisher Scientific, 34578), and, then, blots were imaged using the ChemiDoc XRS system (Bio-Rad, Hercules, CA, USA).

Statistical analysis

Statistical analysis was performed using Graphpad Prism. Data are presented as mean ± SD. $p < 0.05$ indicated statistical significance.

Disclosure statement

No potential conflict of interest was reported by the authors.

Funding

This work was supported by the National Natural Science Foundation of China [No. 31530075] and the National Science and Technology Major Project in New Varieties Cultivation of Transgenic Organisms [2016ZX08007-003].

References

[1] Kabbage M, Dickman MB. The BAG proteins: a ubiquitous family of chaperone regulators. Cell Mol Life Sci. 2008 May;65 (9):1390–1402. PubMed PMID: 18264803.
[2] Wu YY, Guo ZK, Yao KZ, et al. The transcriptional foundations of Sp110-mediated macrophage (RAW264.7) resistance to mycobacterium tuberculosis H37Ra. Sci Rep. 2016 Feb 25;6:22041. PubMed PMID: 26912204; PubMed Central PMCID: PMCPMC4766572.
[3] Wu. Y, Guo Z, Liu F, et al. Sp110 enhances macrophage resistance to *mycobacterium tuberculosis* via inducing endoplasmic reticulum stress and inhibiting anti-apoptotic factors. Oncotarget. 2017. DOI: 10.18632/oncotarget.19300.
[4] Leu JS, Chen ML, Chang SY, et al. SP110b controls host immunity and susceptibility to tuberculosis. Am J Respir Crit Care Med. 2017 Feb 1;195(3):369–382. PubMed PMID: 27858493; PubMed Central PMCID: PMCPMC5328177.
[5] Yao. K, Chen Q, Wu Y, et al. Unphosphorylated STAT1 represses apoptosis in macrophages during *Mycobacterium Tuberculosis* infection. J Cell Sci. 2017;130:1740–1751.
[6] Yang K-M, Bae E, Ahn SG, et al. Co-chaperone BAG2 determines the pro-oncogenic role of cathepsin B in triple-negative breast cancer cells. Cell Rep. 2017;21(10):2952–2964.
[7] Yue X, Zhao Y, Liu J, et al. BAG2 promotes tumorigenesis through enhancing mutant p53 protein levels and function. Elife. 2015 Aug 13;4. PubMed PMID: 26271008; PubMed Central PMCID: PMCPMC4561369. DOI:10.7554/eLife.08401.
[8] Abuaita BH, Burkholder KM, Boles BR, et al. The endoplasmic reticulum stress sensor inositol-requiring Enzyme 1alpha augments bacterial killing through sustained oxidant production. MBio. 2015 Jul 14;6(4):e00705. PubMed PMID: 26173697; PubMed Central PMCID: PMCPMC4502229.
[9] Lim YJ, Choi JA, Lee JH, et al. Mycobacterium tuberculosis 38-kDa antigen induces endoplasmic reticulum stress-mediated apoptosis via toll-like receptor 2/4. Apoptosis. 2015 Dec 28;20(3):358–370.
[10] Moretti J, Roy S, Bozec D, et al. STING senses microbial viability to orchestrate stress-mediated autophagy of the endoplasmic reticulum. Cell. 2017 Nov 2;171(4):809–823 e13. PubMed PMID: 29056340; PubMed Central PMCID: PMCPMC5811766.
[11] Kim KH, Lee MS. Autophagy–a key player in cellular and body metabolism. Nat Rev Endocrinol. 2014 Jun;10(6):322–337. PubMed PMID: 24663220. .
[12] Wang XJ, Yu J, Wong SH, et al. A novel crosstalk between two major protein degradation systems: regulation of proteasomal activity by autophagy. Autophagy. 2013 Oct;9(10):1500–1508. PubMed PMID: 23934082.
[13] Deretic V. Autophagy: an emerging immunological paradigm. J Immunol. 2012 Jul 1;189(1):15–20. PubMed PMID: 22723639; PubMed Central PMCID: PMCPMC3382968. .
[14] Pilli M, Arko-Mensah J, Ponpuak M, et al. TBK-1 promotes autophagy-mediated antimicrobial defense by controlling autophagosome maturation. Immunity. 2012 Aug 24;37(2):223–234. PubMed PMID: 22921120; PubMed Central PMCID: PMCPMC3428731.
[15] Martyniszyn L, Szulc-Dabrowska L, Boratynska-Jasinska A, et al. Crosstalk between autophagy and apoptosis in RAW 264.7 macrophages infected with ectromelia orthopoxvirus. Viral Immunol. 2013 Oct;26(5):322–335. PubMed PMID: 24116707; PubMed Central PMCID: PMCPMC3797454.
[16] Zhang J, He Z, Xiao W, et al. Overexpression of BAG3 attenuates hypoxia-induced cardiomyocyte apoptosis by inducing autophagy. Cell Physiol Biochem. 2016;39(2):491–500. PubMed PMID: 27383426.
[17] Sebti S, Prebois C, Perez-Gracia E, et al. BAG6/BAT3 modulates autophagy by affecting EP300/p300 intracellular localization. Autophagy. 2014 Jul;10(7):1341–1342. PubMed PMID: 24852146; PubMed Central PMCID: PMCPMC4203559.
[18] Bernales S, Schuck S, Walter P. ER-phagy: selective autophagy of the endoplasmic reticulum. Autophagy. 2007 May-Jun;3 (3):285–287. PubMed PMID: 17351330.
[19] Yang L, McBurney D, Tang SC, et al. A novel role for Bcl-2 associated-athanogene-1 (Bag-1) in regulation of the endoplasmic

reticulum stress response in mammalian chondrocytes. J Cell Biochem. 2007 Oct 15;102(3):786–800. PubMed PMID: 17546604.
[20] Gupta MK, Tahrir FG, Knezevic T, et al. GRP78 interacting partner bag5 responds to ER stress and protects cardiomyocytes from ER stress-induced apoptosis. J Cell Biochem. 2016 Aug;117 (8):1813–1821. PubMed PMID: 26729625; PubMed Central PMCID: PMCPMC4909508.
[21] Choi JA, Lim YJ, Cho SN, et al. Mycobacterial HBHA induces endoplasmic reticulum stress-mediated apoptosis through the generation of reactive oxygen species and cytosolic Ca2+ in murine macrophage RAW 264.7 cells. Cell Death Dis. 2013 Dec 12;4: e957. PubMed PMID: 24336077; PubMed Central PMCID: PMCPMC3877560.
[22] Choi HH, Shin DM, Kang G, et al. Endoplasmic reticulum stress response is involved in Mycobacterium tuberculosis protein ESAT-6-mediated apoptosis. FEBS Lett. 2010 Jun 3;584 (11):2445–2454. PubMed PMID: 20416295.
[23] Lim YJ, Choi JA, Choi HH, et al. Endoplasmic reticulum stress pathway-mediated apoptosis in macrophages contributes to the survival of Mycobacterium tuberculosis. PLoS One. 2011;6(12): e28531. PubMed PMID: 22194844; PubMed Central PMCID: PMCPMC3237454.
[24] Fouillet A, Levet C, Virgone A, et al. ER stress inhibits neuronal death by promoting autophagy. Autophagy. 2012 Jun;8 (6):915–926. PubMed PMID: 22660271; PubMed Central PMCID: PMCPMC3427257.
[25] Ding WX, Ni HM, Gao W, et al. Differential effects of endoplasmic reticulum stress-induced autophagy on cell survival. J Biol Chem. 2007 Feb 16;282(7):4702–4710. PubMed PMID: 17135238.
[26] Rikiishi H. Novel insights into the interplay between apoptosis and autophagy. Int J Cell Biol. 2012;2012:317645. PubMed PMID: 22496691; PubMed Central PMCID: PMCPMC3312193.
[27] Deegan S, Saveljeva S, Gorman AM, et al. Stress-induced self-cannibalism: on the regulation of autophagy by endoplasmic reticulum stress. Cell Mol Life Sci. 2013 Jul;70(14):2425–2441. PubMed PMID: 23052213.
[28] Yang H, Ni HM, Guo F, et al. Sequestosome 1/p62 protein is associated with autophagic removal of excess hepatic endoplasmic reticulum in mice. J Biol Chem. 2016 Sep 2;291(36):18663–18674. PubMed PMID: 27325701; PubMed Central PMCID: PMCPMC5009243.
[29] Lamark T, Perander M, Outzen H, et al. Interaction codes within the family of mammalian Phox and Bem1p domain-containing proteins. J Biol Chem. 2003 Sep 5;278(36):34568–34581. PubMed PMID: 12813044.
[30] Kirkin V, Lamark T, Sou YS, et al. A role for NBR1 in autophagosomal degradation of ubiquitinated substrates. Mol Cell. 2009 Feb 27;33(4):505–516. PubMed PMID: 19250911.
[31] Ichimura Y, Kumanomidou T, Sou YS, et al. Structural basis for sorting mechanism of p62 in selective autophagy. J Biol Chem. 2008 Aug 15;283(33):22847–22857. PubMed PMID: 18524774.
[32] Dai Q, Qian SB, Li HH, et al. Regulation of the cytoplasmic quality control protein degradation pathway by BAG2. J Biol Chem. 2005 Nov 18;280(46):38673–38681. PubMed PMID: 16169850.
[33] Ponpuak M, Davis AS, Roberts EA, et al. Delivery of cytosolic components by autophagic adaptor protein p62 endows autophagosomes with unique antimicrobial properties. Immunity. 2010 Mar 26;32(3):329–341. PubMed PMID: 20206555; PubMed Central PMCID: PMCPMC2846977.
[34] Lian J, Wu X, He F, et al. A natural BH3 mimetic induces autophagy in apoptosis-resistant prostate cancer via modulating Bcl-2–Beclin1 interaction at endoplasmic reticulum. Cell Death Differ. 2010;18(1):60–71.
[35] He C, Zhu H, Li H, et al. Dissociation of Bcl-2-Beclin1 complex by activated AMPK enhances cardiac autophagy and protects against cardiomyocyte apoptosis in diabetes. Diabetes. 2013 Apr;62(4):1270–1281. PubMed PMID: 23223177; PubMed Central PMCID: PMCPMC3609561.
[36] Pattingre S, Tassa A, Qu X, et al. Bcl-2 antiapoptotic proteins inhibit Beclin 1-dependent autophagy. Cell. 2005 Sep 23;122 (6):927–939. PubMed PMID: 16179260.
[37] Maiuri MC, Criollo A, Tasdemir E, et al. BH3-only proteins and BH3 mimetics induce autophagy by competitively disrupting the interaction between Beclin 1 and Bcl-2/Bcl-XL. Autophagy. 2014;3 (4):374–376.
[38] Shimizu S, Kanaseki T, Mizushima N, et al. Role of Bcl-2 family proteins in a non-apoptotic programmed cell death dependent on autophagy genes. Nat Cell Biol. 2004 Dec;6(12):1221–1228. PubMed PMID: 15558033.
[39] Malhotra JD, Kaufman RJ. The endoplasmic reticulum and the unfolded protein response. Semin Cell Dev Biol. 2007 Dec;18 (6):716–731. PubMed PMID: 18023214; PubMed Central PMCID: PMCPMC2706143.
[40] Walter P, Ron D. The unfolded protein response: from stress pathway to homeostatic regulation. Science. 2011 Nov 25;334 (6059):1081–1086. PubMed PMID: 22116877.
[41] Grootjans J, Kaser A, Kaufman RJ, et al. The unfolded protein response in immunity and inflammation. Nat Rev Immunol. 2016 Aug;16(8):469–484. PubMed PMID: 27346803; PubMed Central PMCID: PMCPMC5310224.
[42] Lim YJ, Yi MH, Choi JA, et al. Roles of endoplasmic reticulum stress-mediated apoptosis in M1-polarized macrophages during mycobacterial infections. Sci Rep. 2016 Nov 15;6:37211. PubMed PMID: 27845414; PubMed Central PMCID: PMCPMC5109032.
[43] Zhang K, Kaufman RJ. From endoplasmic-reticulum stress to the inflammatory response. Nature. 2008 Jul 24;454(7203):455–462. PubMed PMID: 18650916; PubMed Central PMCID: PMCPMC2727659. .
[44] Gardner BM, Pincus D, Gotthardt K, et al. Endoplasmic reticulum stress sensing in the unfolded protein response. Cold Spring Harbor Perspect Biol. 2013;5(3):a013169–a013169.
[45] Tabas I, Ron D. Integrating the mechanisms of apoptosis induced by endoplasmic reticulum stress. Nat Cell Biol. 2011 Mar;13 (3):184–190. PubMed PMID: 21364565; PubMed Central PMCID: PMCPMC3107571. .
[46] Iurlaro R, Munoz-Pinedo C. Cell death induced by endoplasmic reticulum stress. Febs J. 2016 Jul;283(14):2640–2652. PubMed PMID: 26587781.
[47] Ogata M, Hino S, Saito A, et al. Autophagy is activated for cell survival after endoplasmic reticulum stress. Mol Cell Biol. 2006 Dec;26(24):9220–9231. PubMed PMID: 17030611; PubMed Central PMCID: PMCPMC1698520.
[48] Khaminets A, Heinrich T, Mari M, et al. Regulation of endoplasmic reticulum turnover by selective autophagy. Nature. 2015 Jun 18;522(7556):354–358. PubMed PMID: 26040720.
[49] Marquez RT, Xu L. Bcl-2: beclin 1 complex: multiple, mechanisms regulating autophagy/apoptosis toggle switch. Am J Cancer Res. 2012 Feb 15;2(2):214–221. PubMed Central PMCID: PMCPMC3304572.
[50] Erlich S, Mizrachy L, Segev O, et al. Differential interactions between Beclin 1 and Bcl-2 family members. Autophagy. 2014;3 (6):561–568.
[51] Zhou F, Yang Y, Xing D. Bcl-2 and Bcl-xL play important roles in the crosstalk between autophagy and apoptosis. Febs J. 2011 Feb;278(3):403–413. PubMed PMID: 21182587.
[52] Swerdlow S, Distelhorst CW. Bcl-2-regulated calcium signals as common mediators of both apoptosis and autophagy. Dev Cell. 2007 Feb;12(2):178–179. PubMed PMID: 17276336.
[53] Subramanian M, Shaha C. Up-regulation of Bcl-2 through ERK phosphorylation is associated with human macrophage survival in an estrogen microenvironment. J Immunol. 2007;179 (4):2330–2338.
[54] Park KJ, Lee SH, Lee CH, et al. Upregulation of Beclin-1 expression and phosphorylation of Bcl-2 and p53 are involved in the JNK-mediated autophagic cell death. Biochem Biophys Res Commun. 2009 May 15;382(4):726–729. PubMed PMID: 19318089.

[55] Wei Y, Pattingre S, Sinha S, et al. JNK1-mediated phosphorylation of Bcl-2 regulates starvation-induced autophagy. Mol Cell. 2008 Jun 20;30(6):678–688. PubMed PMID: 18570871; PubMed Central PMCID: PMCPMC2478643.

[56] Smith MD, Wilkinson S. CCPG1, a cargo receptor required for reticulophagy and endoplasmic reticulum proteostasis. Autophagy. 2018;14(6):1090–1091. PubMed PMID: 29916296; PubMed Central PMCID: PMCPMC6103402.

[57] Fumagalli F, Noack J, Bergmann TJ, et al. Translocon component Sec62 acts in endoplasmic reticulum turnover during stress recovery. Nat Cell Biol. 2016 11;18(11):1173–1184. PubMed PMID: 27749824; eng.

[58] Hetz C. The unfolded protein response: controlling cell fate decisions under ER stress and beyond. Nat Rev Mol Cell Biol. 2012 Jan 18;13(2):89–102. PubMed PMID: 22251901. .

[59] Yoshida H, Matsui T, Yamamoto A, et al. XBP1 mRNA is induced by ATF6 and spliced by IRE1 in response to ER stress to produce a highly active transcription factor. Cell. 2001 Dec 28;107(7):881–891.

[60] Cubillos-Ruiz JR, Bettigole SE, Glimcher LH. Molecular pathways: immunosuppressive roles of IRE1alpha-XBP1 signaling in dendritic cells of the tumor microenvironment. Clin Cancer Res. 2016 May 1;22(9):2121–2126. PubMed PMID: 26979393; PubMed Central PMCID: PMCPMC4854763.

[61] Margariti A, Li H, Chen T, et al. XBP1 mRNA splicing triggers an autophagic response in endothelial cells through BECLIN-1 transcriptional activation. J Biol Chem. 2013 Jan 11;288(2):859–872. PubMed PMID: 23184933; PubMed Central PMCID: PMCPMC3543035.

[62] Kouroku Y, Fujita E, Tanida I, et al. ER stress (PERK/eIF2alpha phosphorylation) mediates the polyglutamine-induced LC3 conversion, an essential step for autophagy formation. Cell Death Differ. 2007 Feb;14(2):230–239. PubMed PMID: 16794605.

[63] Kalvakolanu DV, Gade P. IFNG and autophagy: a critical role for the ER-stress mediator ATF6 in controlling bacterial infections. Autophagy. 2012 Nov;8(11):1673–1674. PubMed PMID: 22874566; PubMed Central PMCID: PMCPMC3494595.

[64] Hetz C, Thielen P, Matus S, et al. XBP-1 deficiency in the nervous system protects against amyotrophic lateral sclerosis by increasing autophagy. Genes Dev. 2009 Oct 1;23(19):2294–2306. PubMed PMID: 19762508; PubMed Central PMCID: PMCPMC2758741.

[65] Adolph TE, Tomczak MF, Niederreiter L, et al. Paneth cells as a site of origin for intestinal inflammation. Nature. 2013 Nov 14;503(7475):272–276. PubMed PMID: 24089213; PubMed Central PMCID: PMCPMC3862182.